

# Ultra-low Cost THz Short-range Wireless Link

Stepan Lucyszyn, Hanchao Lu and Fangjing Hu

Department of Electrical and Electronic Engineering

Imperial College London

London, United Kingdom

s.lucyszyn@imperial.ac.uk

**Abstract**—This paper demonstrates an ultra-low cost THz system for implementing a short-range wireless communications link in the far/mid-infrared parts of the electromagnetic spectrum. The basic prototype front-end hardware is deliberately kept very simple; based around miniature incandescent light bulbs, THz filters and pyroelectric infrared sensors. While only a low data rate has been experimentally demonstrated so far, this does not represent a fundamental limitation, as a number of technological enhancements are possible. It is believed that this “THz torch” technology has its niche in ubiquitous security applications that do not require high data rates or large distance operation (e.g. secure RFID, smart key fobs and remote controls).

**Keywords-component; low cost; THz, wireless link, RFID, fob**

## I. INTRODUCTION

Terahertz systems are notoriously very expensive, from complete systems down to individual active devices and passive components. For this reason, there are very few ubiquitous commercial applications in the far-infrared (300 GHz to 30 THz) and mid-infrared (30 THz to 120 THz) parts of the electromagnetic spectrum; notable exceptions to this are relatively basic ultra-low cost human body detection systems (for applications ranging from security to energy-saving lighting systems) and fire detection systems.

An example of an ultra-low cost wireless communications system can be found in ubiquitous near-infrared remote controls, which operate at a wavelength of 940 nm (i.e. 319 THz). This technology has been around since the early 1980s. However, to date, there has been no reported R&D into similar systems at longer wavelengths.

To this end, this paper reports on an ultra-low cost technology that operates between 25 and 50 THz, using simple ON-OFF keying digital modulation. The basic architecture for this “THz torch” system is shown in Fig. 1.

## II. EXPERIMENTAL PROOF-OF-CONCEPT DEMONSTRATOR

### A. Ultra-low Cost THz Transmitter

The “THz torch” transmitter employs simple incandescent light bulbs to generate incoherent electromagnetic energy by thermal emission. In order for the peak spectral power density to be located in the far/mid-infrared parts of the electromagnetic spectrum, the filament needs to be able to get hot. Of all metals in their purest form, tungsten has the highest melting point of 3,695 K. For this reason, tungsten bulbs are the preferred choice for this application (e.g. the miniature 400 mW Eiko 8666-40984, shown in Fig. 2(a)).

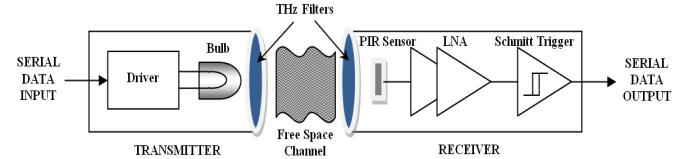


Figure 1. Architecture for basic ultra-low cost ON-OFF keying “THz torch” wireless communications links (optional parabolic reflectors/collimator lenses are not shown)

Ideal blackbody thermal emission intensity, as a function of wavelength, can be obtained using Planck’s Law, if the temperature of the tungsten filament is known. To this end, a simple test circuit, shown in Fig. 2(b) was used to determine the working temperature of a single bulb, to a first degree of approximation.

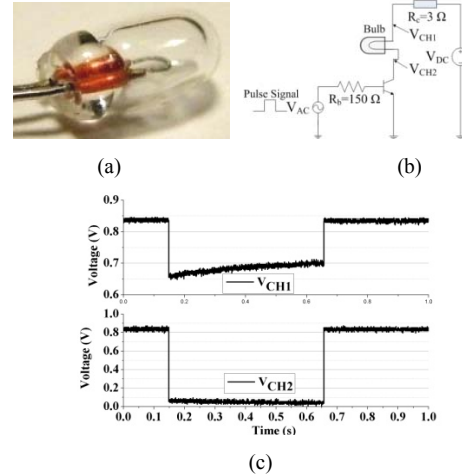


Figure 2. Evaluating the temperature of the tungsten bulbs (a) Eiko 8666-40984 incandescent bulb (diameter = 2.6 mm, length = 6.3 mm); (b) test circuit (and transmitter driver circuit with  $R_C = 3 \Omega$ ); and (c) measured voltages  $V_{CH1}$  (upper trace) and  $V_{CH2}$  (lower trace)

The turn-ON thermal time constant is defined here as the time it takes to go from 10% to 90% of the final steady-state temperature. From Fig. 2(c), with the rising edge of the input pulse, the voltage output  $V_{CH1}$  falls from  $V_{DC} = 0.839$  V down to 0.652 V and then rises to the steady-state value of 0.705 V. This relatively slow response is due to the turn-ON thermal time constant of the complete circuit being  $\sim 320$  ms (*c.f.* the electrical time constants within this circuit being many orders of magnitude shorter). It has been found that the turn-ON thermal time constant for the single bulb (i.e. without any additional collector resistance,  $R_C$ ) is 155 ms.

This work was funded by the UK Engineering and Physical Science Research Council (EPSRC), under Platform Grant EP/E063500/1

Using an *RLC* meter, at a room temperature of  $T_0 = 300$  K, a single non-biased bulb can be represented by the measured series resistance and inductance values of  $R_b(300\text{ K}) = 4.62\ \Omega$  and  $L_b = 5.04\ \mu\text{H}$ , respectively, giving an electrical time constant of only  $1.08\ \mu\text{s}$ . For a tungsten bulb, the resistivity [1] of its filament can be represented by the following:

$$\begin{aligned}\rho(T) &= 6.843 \times 10^{-12} T^2 + 1.879 \times 10^{-8} T - 8.138 \times 10^{-8} \\ \text{for } T > 200\text{ K} \\ \rho(T) &= R_b(T) \cdot CSA/l\end{aligned}\quad (1)$$

where  $T$  is the absolute temperature of the filament, having the following parameters:  $CSA = \text{cross-sectional area } [\text{cm}^2]$  and  $l = \text{length } [\text{cm}]$ . At 300 K, a value of  $CSA/l = 1.177 \times 10^{-6}\ \text{cm}$  can be extracted.

Now, unlike its series inductance, the resistance of the tungsten bulb changes with temperature. The steady-state current through and voltage across the single bulb are 44 mA and 665 mV, respectively, giving a steady-state resistance  $R_b(T) = 15.09\ \Omega$  at this bias point. Using (1), an absolute temperature of  $T = 772$  K can be extracted, to a first order of approximation. By employing Wien's Displacement Law, which gives the inverse relationship between the wavelength of peak emission  $\lambda_{max}$  [m] and blackbody temperature  $T_{bb} \sim T$  [K] as [2, 3]:

$$\lambda_{max} = b/T_{bb} \sim 3.75\ \mu\text{m} \quad (2)$$

where the constant of proportionality,  $b = 2.8978 \times 10^{-3}$  [m.K]. Therefore, the spectral peak is at  $\sim 80$  THz at this bias point, for a DC power dissipation of 29.3 mW in the bulb (i.e. operating at only 7% of its maximum rated power level).

The thermal radiation can now be calculated and plotted, as shown in Fig. 3 for the steady-state, using Planck's law of blackbody radiation [3]. The spectral radiance of un-polarized electromagnetic radiation at all wavelengths emitted from a black body at absolute temperature  $T$  is given by:

$$I(v, T) = \frac{2hv^3}{c^2} \frac{1}{e^{hv/kT} - 1} \quad (3)$$

where  $I(v, T)$  is the power radiated per unit area of emitting surface in the normal direction per unit solid angle per unit frequency by a black body;  $h$  is Planck's constant;  $c$  is the speed of light in vacuum;  $k$  is Boltzmann's constant; and  $v$  is the frequency of the electromagnetic radiation.

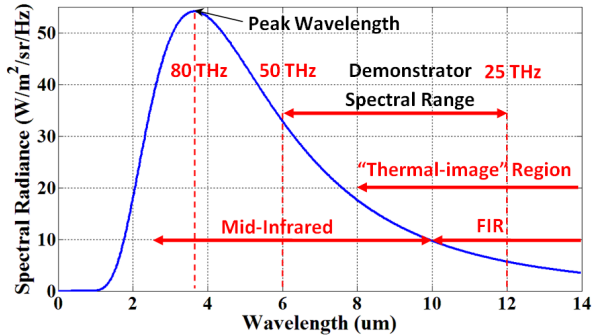


Figure 3. Calculated steady-state spectral radiance against wavelength at 772 K

Using 5 bulbs in series, to maximize data rate and output power, the assembly of the THz transmitter front end is shown in Fig. 4.

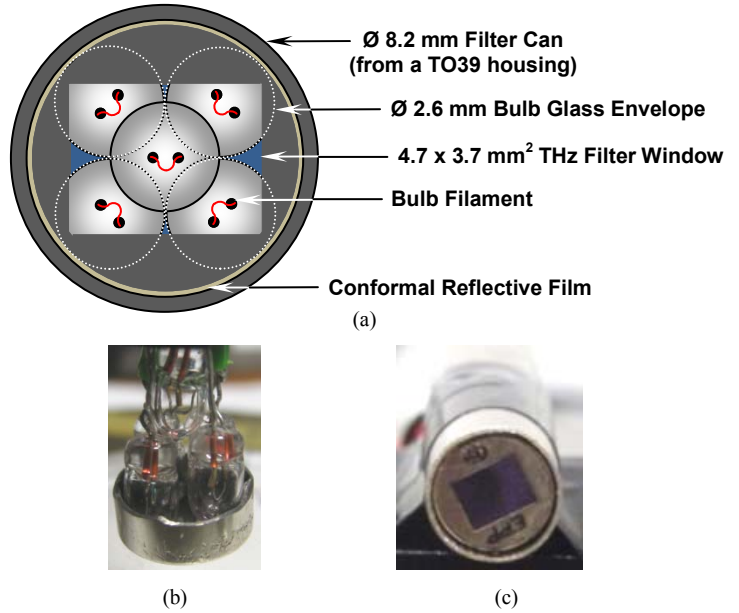


Figure 4. THz Transmitter front end (a) illustration of assembly (looking from behind); (b) photograph of assembled front end (conformal reflective film removed); (c) complete THz transmitter in  $\phi$  1 cm package

#### B. Ultra-low Cost Bandpass Filter

A simple filter was employed in both transmitter and receiver front ends, using commercially-available 5 to 14  $\mu\text{m}$  long wave pass silicon optical filters [4], having a spectral transmittance response given in Fig. 5. In the frequency range from 25 to 50 THz, the transmittance is  $>70\%$ . Since the peak spectral radiance is at 80 THz, for a dissipated power of 29.3 mW, it may be possible to bring this down to  $\sim 40$  THz (i.e. into the spectral range of the filter's pass band) by significantly decreasing the DC power dissipated. This will give the added benefits of a significantly longer lifetime of battery operation and also results in a substantial increase in the mean-time-to-failure (i.e. the working lifetime) of the bulb.

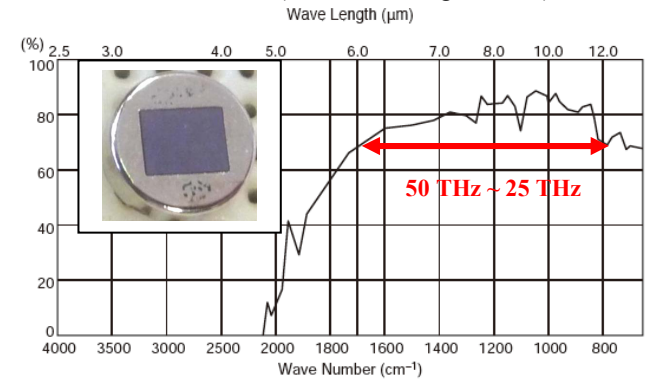


Figure 5. Spectral transmittance response [4] of 5 to 14  $\mu\text{m}$  long wave pass silicon optical filter, having a 5.5  $\mu\text{m}$  cut-off wavelength at 50% transmittance (with inset photograph showing the 4.7 x 3.7  $\text{mm}^2$  filter window)

For narrower fractional bandwidths of operation (e.g. between 10% and 30%), metal mesh resonant filters can also be employed, as demonstrated by a 14% fractional bandwidth filter at 10 THz, patterned by a 2-dimensional array of half-wavelength sized crosses (15  $\mu\text{m}$  in size) [5]. At 40 THz, the half-wavelength size of 3.75  $\mu\text{m}$  is very close to the 1  $\mu\text{m}$  minimum feature size limit for low-cost shadow mask manufacturing.

### C. Ultra-low Cost THz Receiver

The pyroelectric infrared (PIR) sensor is becoming more and more ubiquitous, as it can be used for human body and fire detection systems. It is able to detect targets by measuring the difference in temperature between a target object and its background. Because of their relatively simple manufacturing technology and high-volume markets, they are relatively ultra-low cost devices and can even include integrated Fresnel lenses. With operation in the 5 to 14  $\mu\text{m}$  wavelength range, it is ideal for “THz torch” receiver applications. For this reason, the Murata Manufacturing Co. IRA-E710ST1 dual-type PIR [4] was employed for detecting the THz radiation generated by the incandescent bulbs, as shown in Fig. 6 (45° field of view and typical sensitivity of 4.3 mVp-p). Note that, in order to use the PIR sensor as an ON-OFF keying modulation detector, one of the two passive pyroelectric elements had to be shorted out.

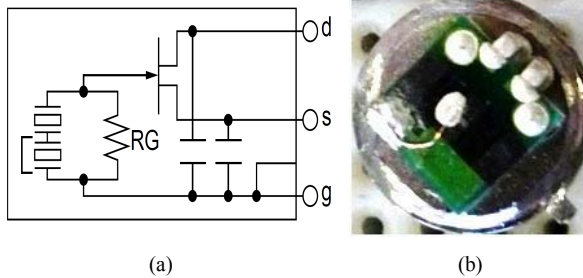


Figure 6. (a) internal circuit of Murata IRA-E710ST1 dual-type PIR sensor [4]; and (b) photograph of the sensor (showing one of the passive pyroelectric elements being shorted out)

The analogue circuitry of the receiver consists of a 2-stage very high gain (100 dB) low-noise amplifier (LNA), employed for signal amplification (and DC blocking) with LM358 operational amplifiers, and an output voltage comparator (using a Schmitt trigger). With the latter stage, the output is switched negative when the input passes upward beyond a positive threshold voltage. It then uses negative feedback to prevent switching back to the other state until the input passes through a lower threshold voltage, thus stabilizing the switching against rapid triggering by noise as it passes the trigger point. This is an important consideration, as the PIR sensor elements can be sensitive to external noise sources.

In order to use the PIR sensor for implementing ON-OFF keying modulation detection, it is necessary to consider its sensitivity and relative responsivity to the chopping frequency (i.e. the data rate in this application). With reference to Fig. 7, it can be seen that there will be nearly an order of magnitude reduction in responsivity per decade increase in data rate. Therefore, only low data rates (e.g. of the order of 10 bps) can be supported by the Murata IRA-E710ST1 PIR sensor.

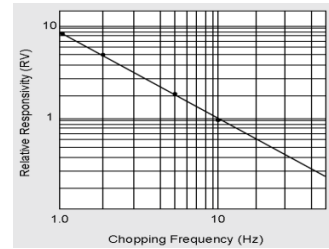


Figure 7. Relative responsivity of Murata IRA-E710ST1 PIR sensor [4]

### D. Ultra-low Cost THz Wireless Communications Link

The complete system illustrated in Fig. 1 was assembled and the transmitter and receiver were positioned 0.5 cm apart to create a line-of-sight wireless communications link. The results of the measured effective bit rate for the end-to-end link, for different numbers of bulbs connected in series, can be seen in Fig. 8; with 5 bulbs giving a 5.11 bps link.

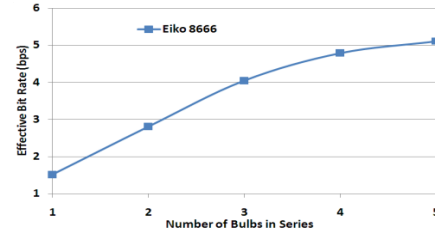


Figure 8. Maximum effective bit rate against number of Eiko 8666-40984 bulbs connected in series (each with a DC power dissipation of 29.3 mW)

The corresponding receiver's output voltage for this link can be seen in Fig. 9. With the transmitted pulses being recovered by the receiver, this result clearly shows that the proof-of-concept prototype demonstrator works for low data rates and over short distances. The effective bit rate against distance, for this 5-bulb transmitter, is shown in Fig. 10. The overall end-to-end bit rate is limited by the turn-ON and turn-OFF thermal time constants for both incandescent bulb and PIR sensor, as well as the detectivity, sensitivity and relative responsivity of the PIR sensor. Therefore, while this first proof-of-concept prototype demonstrator may have a limited performance there is ample scope for improvement.

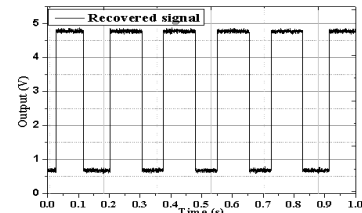


Figure 9. Receiver output voltage showing the recovered 5.11 bps signal

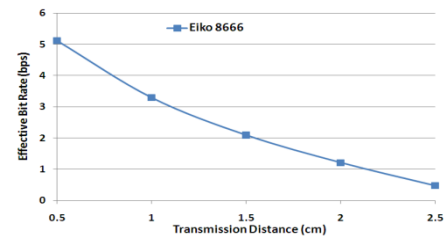


Figure 10. Maximum effective bit rate against distance for 5 Eiko 8666-40984 bulbs connected in series (each with a DC power dissipation of 29.3 mW)

### III. DISCUSSION

When a rectangular pulse generator is used to create the input baseband signal, the shorter the duration of the pulse the lower the filament's temperature increases during that pulse. Also, the peak temperature will vary with the corresponding duty cycle of the rectangular pulse train. The peak temperature will generally be less if the current through the bulb has a lower Mark-Space ratio, as illustrated in Fig. 11. Thus, the duty cycle is an important factor for a long thermal time constant system. This phenomenon could be exploited, to create a more DC power efficient transmitters, using asynchronous signaling.

The incident electromagnetic pulse at the PIR sensor may become undetectable if its energy results in a change in temperature that is too small to detect. One very important advantage of this basic technology is that the spectral peak can be made tunable, by simply controlling the current through the bulb. For sensors that measure a change in temperature, the spectral peak can be swept in time, using a dynamic bias control scheme, to increase both data rate and transmitter DC power efficiency.

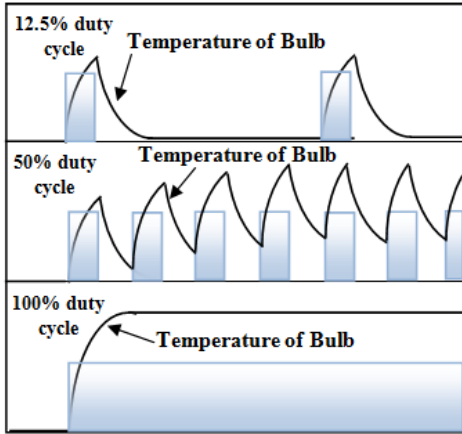


Figure 11. Effect of duty cycle on coil (or filament) temperature [6]

Alternatively, a much faster mechanical or liquid crystal modulator can be employed to pulse the electromagnetic energy from a continuously illuminated incandescent bulb. This solution has the advantage of being able to support much higher data rates, which would now be limited by the thermal time constant of the passive PIR sensor element or electrical time constant of an active device.

The InfraTec LME-337 [7] is a fast infrared pyroelectric detector that has a typical thermal time constant of 150 ms, offers a minimum RMS voltage responsivity of 140 V/mW at a 10 Hz chopping frequency with a typical -3(-6) dB roll off at 40(70) Hz. More importantly, within its TO39 housing, it has an integrated advanced transimpedance amplifier specifically designed for a 1 to 100 Hz modulation frequency range, with  $2.0 \times 10^8 \text{ cm} \cdot \text{Hz}^{1/2} / \text{W}$  detectivity at a 70 Hz chopping frequency. In addition, the LIE-312 [7] has a  $1.0 \times 10^8 \text{ cm} \cdot \text{Hz}^{1/2} / \text{W}$  detectivity at a 1 KHz chopping frequency, albeit it with a 200 ms thermal time constant and minimum RMS voltage responsivity of 0.5 V/mW at a 10 Hz chopping frequency.

### IV. CONCLUSIONS

This paper has introduced an ultra-low cost THz system for implementing a short-range wireless communications link in the far/mid-infrared parts of the frequency spectrum. While the measured performance, to date, has been rather limited, in terms of data rate and range, a number of recommendations have been given for further investigation.

The proposed technology has the benefits of: (1) being very easy to manufacture in large volumes; (2) inherently ultra-low cost; (3) providing tuneable spectral peaks; (4) having an array of alternative enabling technology solutions; and (5) because it operates in a virtually unused part of the frequency spectrum, offers covert operation for security applications. For these reasons, it is believed that this first working prototype proof-of-concept demonstrator will serve as inspiration for further research and development into similar systems architectures, while potentially opening up this part of the frequency spectrum to more ubiquitous commercial applications.

This "THz torch" technology is expected to have its niche in security applications that do not require high data rates but must be low cost (e.g. secure RFID, smart key fobs and remote controls). This is because, with such large amounts of freely available spectrum and high atmospheric attenuation, there is an extremely low probability of intercept and code grabbing.

To increase data rates and make the link more robust to interference, frequency division multiplexing (FDM) can be introduced, where an input data stream is split into various channels and each channel is transmitted within different spectral frequency bands within the mid-infrared region. Alternatively, a frequency-hopping spread spectrum (FHSS) system can be realized to further increase the level of security, where data is transmitted at different times within predetermined spectral frequency bands within the mid-infrared region. With both FDM and FHSS applications, InfraTec offers a wide range of standard narrow band pass (NBP) filters and windows that were originally developed for gas analysis. For example, filters with band pass centers at 41, 56, 63, 67, 70, 76 and 88 THz already exist [8] and these can be readily employed to create a 7-channel filter bank for FDM/FHSS applications.

### REFERENCES

- [1] D. A. Clauss, R. M. Ralich, and R. D. Ramsier, "Hysteresis in a light bulb: connecting electricity and thermodynamics with simple experiments and simulations", Eur. J. Phys., vol. 22 , pp. 385–394, 2001
- [2] M. Lianxi, Y. Junjun, N. Jiabei, "Tungsten filament emissivity behavior", Lat. Am. J. Phys. Educ. vol. 3, no. 3, Sept. 2009
- [3] <http://en.wikipedia.org/wiki/Blackbody>
- [4] Murata Manufacturing Co., "Pyroelectric infrared sensor & sensor module", Catalogue No. S21E-2
- [5] A. M. Melo, Mariano A. Kornberg, P. Kaufmann, M. H. Piazzetta, E. C. Bortolucci, M. B. Zakia, O. H. Bauer, A. Poglitsch and A. M. P. Alves da Silva, "Metal mesh resonant filters for terahertz frequencies", Applied Optics, vol. 47, no. 32, pp. 6064-6069, Nov. 2008
- [6] [http://relays.tycoelectronics.com/schrack/pdf/C0\\_v4bg\\_5.pdf](http://relays.tycoelectronics.com/schrack/pdf/C0_v4bg_5.pdf)
- [7] [http://www.infratec.de/en/sensorik/mainmenu/products/detector-search.html?no\\_cache=1](http://www.infratec.de/en/sensorik/mainmenu/products/detector-search.html?no_cache=1)
- [8] <http://www.infratec.de/en/sensorik/mainmenu/products/ir-filter.html>